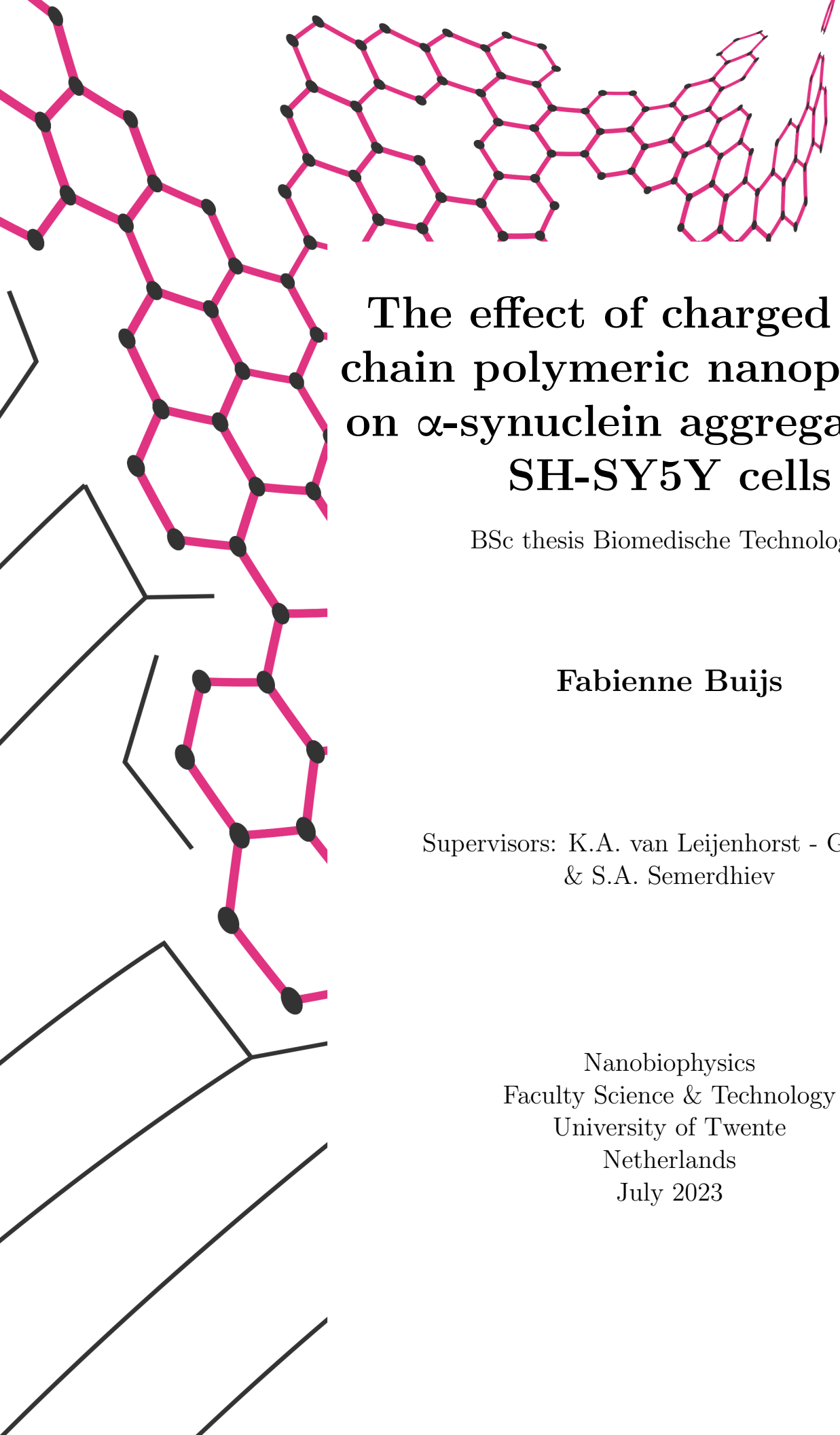

UNIVERSITY OF TWENTE.

The effect of charged single chain polymeric nanoparticles on α-synuclein aggregation in SH-SY5Y cells

BSc thesis Biomedische Technologie

Fabienne Buijs

Supervisors: K.A. van Leijenhorst - Groener
& S.A. Semerdhiev

Nanobiophysics
Faculty Science & Technology
University of Twente
Netherlands
July 2023

Abstract

Parkinson's disease (PD) is an increasing problem, with more than a million cases worldwide. 95% of the cases is sporadic and to decrease the amount of cases, it is important to find what can induce PD. A characteristic of the disease is the aggregation of α-synuclein, causing dopaminergic neurons to die. The aggregation can be caused by positive particles, next to that nanopolymers, produced for controlled drug delivery, with tertiary amine can enter the cytosol where they can reach the α-synuclein. The goal of this research is to find out if these nanopolymers can induce α-synuclein aggregation, in and outside the cell. For this the affinity is researched, just like the aggregation outside the cell and the effect of the nanoparticles on α-synuclein in SH-SY5Y cells. It is shown that nanoparticles with 60% tertiary amine (positively charged) can induce aggregation. The higher the amount of tertiary amine, the faster aggregation occurs and the more toxic the nanoparticles are. Nanoparticles with 0% tertiary amine (negatively charged) limit the aggregation. In SH-SY5Y cells, none of the nanoparticles induce aggregation in 72 hours. This research shows that the nanopolymers can be toxic to the brain and must therefore be handled with care.

Samenvatting

De ziekte van Parkinson (PD) is een groeiend probleem, met wereldwijd meer dan een miljoen diagnoses. 95% van de gevallen is sporadisch en om het aantal gevallen te verminderen, is het belangrijk om te onderzoeken wat PD veroorzaakt. Kenmerkend voor de ziekte is de aggregatie van α-synucleïne, waardoor dopaminerge neuronen afsterven. De aggregatie kan worden veroorzaakt door positieve deeltjes, daarnaast kunnen nanopolymeren, geproduceerd voor gecontroleerde medicijntoediening, die tertiaire amines bevatten in het het cytosol komen, waar ze de α-synucleïne kunnen bereiken. Het doel van dit onderzoek is om uit te zoeken of deze nanopolymeren de aggregatie van α-synucleïne kunnen induceren, zowel binnen als buiten de cel. Hiervoor is de affiniteit onderzocht, evenals de aggregatie buiten de cel en het effect van de nanodeeltjes op α-synucleïne in SH-SY5Y cellen. Het blijkt dat nanodeeltjes met 60% tertiaire amines (positief geladen) aggregatie kunnen veroorzaken. Hoe hoger de hoeveelheid tertiaire amines, hoe sneller de aggregatie optreedt en hoe toxischer de nanodeeltjes zijn. Nanodeeltjes met 0% tertiare amines (negatief geladen) remmen de aggregatie. In SH-SY5Y cellen induceert geen van de nanodeeltjes aggregatie binnen 72 uur. Dit onderzoek toont aan dat nanopolymeren giftig kunnen zijn voor de hersenen en met voorzichtigheid behandeld moeten worden.

Acknowledgements

This bachelor thesis was done at the Nanobiophysics group at the University of Twente, I am thankful for prof. dr. M.M.A.E. Claessens and dr. C. Blum for giving me the opportunity. I want to thank my daily supervisors, dr. ir. S.A. Semerdhiev and ing. K.A. van Leijenhorst-Groener, for their help. Last but not least I am very grateful for having N.I.C.L Han and L.J. Visscher for their relaxing talks and critical view.

Contents

1 Introduction

With more than one million cases worldwide in 2019 and a 160% increase in cases since 1990, Parkinson's disease is an increasing problem [1]. Parkinson's disease (PD) is the second most common neurodegenerative disorder and the incidence greatly increases with age. Due to the loss of dopaminergic neurons in the substantia nigra pars compacta, patients eventually show symptoms like trembling at rest, rigidity, involuntary movement, postural instability and freezing. In the development of PD, oxidative stress, mitochondrial respiration defects and abnormal protein aggregation may be important. Aggregation following the overproduction of α-synuclein, due to a mutation in the gene, causes a genetic form of PD. 95% of the PD cases is however sporadic, meaning that there's no genetic cause. Sporadic PD is probably caused by a combination of environmental and genetic factors, the aggregation of α-synuclein is also involved in this variant [2]. Oxidative damage enhances the misfolding of α-synuclein, meaning the different factors exist together [2]. The aggregation of α-synuclein can be induced by different external influences. One of these factors is nanoparticles [3]. Nanoparticles are however also used to treat PD and can thus possibly have a two-sided, but very conflicting, effect on the cell [4]. This research will be focused on the induced aggregation of α-synuclein by polymeric nanoparticles, which are used for the controlled delivery of drugs.

1.1 A-synuclein

A-synuclein is found in the presynaptic region of the neuron and probably plays a role in exocytosis. The molecule is also able to go in the nucleus of the cell, as it is a small protein [5]. A-synuclein is made out of 140 amino acids and can be divided into three regions: the N-terminal region, the hydrophobic region and the C-terminal region, which is acidic. Overall, the protein is negatively charged, mostly due to the C-terminal. Aggregation of α-synuclein primarily happens when the C-terminal is truncated, decreasing the repulsion between multiple α-synuclein monomers. The protein is *in vitro* not neatly folded like other proteins, but it is part of the intrinsically disordered proteins [6]. In contact with a membrane the protein forms an α-helix. In aggregates, α-synuclein forms intermolecular β-sheets [7].

A-synuclein aggregation results in the formation of amyloid fibrils. The formation of fibrils consists of two stages: nucleation and growth. The aggregation forms a sigmoidal formed binding curve. The curve starts with a plateau, at that point there are only monomers present. The whole process starts with destabilisation of the monomers after which oligomers are formed. The nucleation is the initial binding of the monomers to each other. There are different types of nucleation. Primary nucleation is the initial event in which a nucleus consisting of monomers is formed, this nucleus can grow due to attachment of new monomers or aggulation with other nuclei. New filaments can also be formed via secondary nucleation or fragmentation. In this process new filaments are created from already existing filaments, this speeds up the amyloid fibril formation The lag phase is the first part of the sigmoidal curve, this phase ends with the nucleation after which the degree of aggregation explodes and the growth phase starts. In this phase molecules increase in average length and the curve shows a strong increase. The curve ends with a second plateau when the aggregates are in equilibrium, the average size does not increase from that point on. The aggregation process is a complex process and sensitive to environmental factors [8, 9].

Due to mutations, the amount of α-synuclein can increase, which can lead to aggregation and eventually to PD. A mutation is not the only cause for aggregation, but what exactly causes the aggregation and misfolding is still being researched [5]. In PD, the disrupted function of the mitochondria is probably caused by the aggregation of α-synuclein. Due to the misfunctioning of the mitochondria, the amount of reactive oxygen species increases, making it harder for the cell to survive [7]. The oxidative stress that arises can induce α-synuclein aggregation, leading to a vicious circle. A-synuclein aggregation can thus be caused by an increased amount of monomeric α-synuclein and by oxidative stress, aggregated α-synuclein causes cellular toxicity. Next to that, the aggregations can spread, leading to a progressive spread of the disease [10]. Exosomes may play a role in the spreading of aggregated α-synuclein to other neurons, as the N-terminal domain of α-synuclein binds to membranes [11].

1.2 Effect of nanoparticles on aggregation

Recently, a lot of research has been done in the field of nanomedicine. Polymeric nanoparticles can carry drugs to certain cells, making it possible to lower the drug dose [12]. Even for treating PD, polymeric nanoparticles

are used to replace for example the deficient dopamine in patients [4]. These nanoparticles have benefits, but can also be detrimental to other cells.

Nanoparticles can inhibit or promote aggregation. M. Mahmoudi et al. found that positively charged nanoparticles with a zeta-potential of +9 mV promote aggregation in high concentration. If the nanoparticles are in low concentration they inhibit the aggregation, as the negatively charged α-synuclein binds to the positive particles and is therefore not available for aggregation. In high concentration the α-synuclein clusters can progress into amyloid fibrils easily, due to a high number of proteins being close to each other. For negatively charged particles, the surface area seems to have an effect on the aggregation. A smaller particle (39.7 ± 0.1 nm) has a bigger inhibitory effect on the amyloid formation than a bigger particle (64.6 ± 1.3 nm) [3]. S. Mohammidi et al. found that TiO_2 decreased the lag time for nucleation, meaning aggregates were formed faster and in a greater number. The length of the lag phase is dependent on the amount of nanoparticle. It is also known that TiO_2 induces aggregation via oxidative stress [13]. Preliminary data from the Nanobiophysics group at the University of Twente showed that positively charged nanoparticles trigger the aggregation of α-synuclein into amyloid fibrils.

For nanoparticles to affect the neurons, they should enter the brain. Small nanoparticles can do that [13]. To have an effect on α-synuclein in the braincells, the nanoparticles must enter the cytosol. N.M. Hamelmann et al. showed that single chain nanopolymers with a high amount of tertiary amines, produced for controlled drug delivery, can enter the cytosol and can therefore possibly affect α-synuclein. The nanoparticles enter the cell via endocytosis, after which they can escape the endosome. Due to protonated tertiary amines, chloride ions can enter the endosomes. Upon this, water will enter the endosome and the endosomes will swell, causing them to break. This releases the nanoparticles in the cytosol, instead of in the endosomes [14]. Size also plays an important effect, smaller particles are taken up more than bigger particles, as proven by Y. Bai et al. [15].

Increasing the amount of tertiary amines also means the charge of the particles is more positive. These positively charged nanoparticles can then reach the cytosol, the proteins in the cell are not protected by the endosome anymore. This can be connected to the preliminary data from the Nanobiophysics group stated earlier: α-synuclein is present in the cytosol and positive nanoparticles can go in the cytosol, where they possibly induce aggregation. Therefore, positive nanoparticles can result in aggregation of α-synuclein *in vivo*. To test the ability of positively charged nanoparticles to induce the formation of amyloid fibrils in cells, nanoparticles are added to SH-SY5Y cells (neuroblastoma) in this research.

1.3 SH-SY5Y cells

SH-SY5Y cells are used often in PD research, as they express dopaminergic markers and are derived from a human. The cell line does come from a cancerous model, but most genetic material important in the development of PD is not affected by malignant mutations [16, 17]. The SH-SY5Y cell line is a human neuroblastoma cell line with a doubling time of roughly 27 hours. The cells are non-polarized. SH-SY5Y cultures mostly contain floating and adherent cells, it is possible for the cells to interchange between these two types. The cells can be differentiated, forming a more neuron-like cell and leading to a more homogeneous cell population. The differentiated cells have more characteristics of neurons and execute neuronal processes, these cells are polarized. To differentiate cells, retionoic acid is used most of the times [18].

1.4 Research question and hypothesis

This research will be focused on the effect of charged single chain nanopolymers on α-synuclein in SH-SY5Y cells. For that, the affinity between the nanoparticles and α-synuclein is investigated. It is researched if the nanoparticles can cause aggregation in and outside the cell and what the effect of aggregation on the cell viability is.

It is expected that the positive nanoparticles have affinity for α-synuclein, as the protein is negatively charged. The positive nanoparticles induce aggregation, a more positive particle will induce more aggregation than a less positive nanoparticle. It is hypothesised that the viability of the cells is mostly be affected by the induced aggregation, which is toxic to cells. The cells to which more positive nanoparticles are added are therefore expected to have a decreased viability. Overall it is hypothesised that positively charged polymeric nanoparticles induce aggregation of α-synuclein in SH-SY5Y cells.

2 Materials and Methods

2.1 Nanoparticle production

The nanoparticles are obtained from N.M. Hamelmann et al., produced as stated in their research [14]. For this research three nanoparticles are used: the one with 0%, 30% and 60% tertiary amine. The nanoparticles are pentafluorophenyl-functional single chain polymeric nanoparticles, synthesised via a thiol-Michael reaction. Due to intramolecular crosslinking, they become small [14]. The backbone of the nanoparticles is a copolymer of pentafluorophenyl methacrylate and 2-(ethyl xanthate) ethyl methacrylate in a ratio of 10:1 [19]. The nanoparticles are functionalised with different amounts of tertiary amine (N,N-dimethylethylenediamine), other pentafluorophenyl groups are swapped for 1-aminoglycerol to ensure water solubility. The nanoparticles are labelled with DTAF (5-(4,6-dichlorotriazinyl) aminofluorescein), with an absorption wavelength of 492 nm and an emission wavelength of 516 nm. According to N.M. Hamelmann et al. the nanoparticles have an average size of 12 nm and a zeta-potential of -27 mV, +21 mV and +27 mV for the 0%, 30% and 60% tertiary amine nanoparticles respectively [14]. The nanoparticles are dissolved in 20 mM Tris (pH 7.4, Sigma-Aldrich, UK) in a concentration of 1 mg/mL.

2.2 Nanoparticle characterisation (FCS)

The size of a particle can be determined by fluorescence correlation spectroscopy (FCS). This technique can determine the diffusion speed of a particle, which correlates to the radius. FCS uses a small volume in which the fluorescence fluctuations are measured. These fluctuations are due to fluorophores diffusing through the volume. The autocorrelation function of these fluorescence fluctuations can be fitted to a 3D diffusion model. From this model, the diffusion speed can be found [20].

The FCS is done using the Microtime 200 (PicoQuant, Germany) and analysed with SymPhoTime 64 (PicoQuant, Germany). The excitation wavelength is 485 nm and the fluorescence is measured after the light is filtered through a longpass filter with a cut-on wavelength of 488 nm. Per nanoparticle, 8 measurements are done, each of 120 seconds with a 2 second interval. The FCS analysis is done over the interval 0.01-500 ms, using a second order triplet fit. With the measured diffusion speed the size is calculated, according to the Stokes-Einstein equation:

$$R = \frac{K_B T}{D 6 \pi \eta} \tag{1}$$

In Formula 1 R is the size, K_B the Boltzman constant, T the temperature, D the diffusion speed and η the viscosity of the solvent. The lifetime of the different particles is also analysed, using time-correlated single photon counting (TCSPC). This gives insight in the fluorophore labelling efficiency.

$$\frac{N(t)}{N_0} = e^{-\frac{t}{\tau}} \tag{2}$$

The equation for the exponential decay of the fluorescence ($\frac{N(t)}{N_0}$) is given in Formula 2. The lifetime is given by τ, assuming a single exponential decay. A bigger value of τ thus means a slower decay and a longer lifetime.

The FCS measurement is done for nanoparticles diluted in MilliQ and for nanoparticles diluted in the cell culture medium, in the same concentration that is added to the cells (250 nM). The FCS is measured 24 hours after adding the nanoparticles to the medium and 6 days after adding the nanoparticles to the medium.

2.3 Microscale Thermophoresis

For a particle to have effect on α-synuclein, it should have some binding affinity to the protein. The binding affinity can be measured using microscale thermoporesis (MST), this technique is based on the movement of molecules upon temperature changes. A certain volume is heated with a laser, creating a temperature gradient where molecules move in or out of. The fluorescence of the labelled particles is measured to determine the amount of molecules in that volume. The binding of a particle with α-synuclein creates a complex with a different hydration shell, size and charge. This complex acts different upon temperature changes [21, 22]. There are different ligand concentrations used, to find the binding affinity these are used as the input. The output is the difference in fluorescence between the bound and unbound state. A binding curve can be fitted, with this the binding affinity can be calculated [22].

The binding affinity of the nanoparticles is measured using the Monolith NT.115 (NanoTemper Technologies GmbH, Germany). In this research, three nanoparticles are used. The used nanoparticles consist of 0% tertiary amine, 30% tertiary amine or 60% tertiary amine. The buffer consists of 20 mM Tris and 10 mM NaCl (Sigma-Aldrich, USA). The starting concentration of wild-type α-synuclein (preparation is done by the Nanobiophysics group, as in research of S.A. Semerdzhiev et al. [23]) is 250 nM. A dilution series of 16 solutions is made, diluting 1:1 each time. 10 µL of each dilution is made, to which 10 µL labelled nanoparticle is added. The labelled nanoparticles are added in a concentration of 625 nM, leading to a final concentration of 312.5 nM. After adding everything together, the samples are incubated for 30 minutes and then measured. The samples are measured again after 30 hours, to see if an equilibrium was formed after 30 minutes.

Measurements are split into three steps with increasing MST power. In all measurements, the LED power is 60% and the incident laser is on for five seconds before and after each measurement. The delay is 25 seconds. The MST laser is on for 30 seconds per measurements and the power is 20% for the first measurement, 40% for the second and 80% for the third measurement. Outliers are taken not taken into account for the analysis. A curve is fitted following the K_D model using the MO.Affinity Analysis software (Nanotemper).

2.4 Thioflavin T aggregation assay

To follow the aggregation process, a thioflavin T aggregation assay (ThT assay) is executed. Thioflavin T becomes strongly fluorescent when it is bound to the β-sheets in amyloid fibrils [24]. The ThT assay is performed as described in work from M.M. Wördehoff et al. [25]. The sample solution consists of 20 mM Tris, 5 µM thioflavin T (Fluka, Sigma-Aldrich, UK), 10 mM NaCl, 0.02 w% sodium azide (Sigma-Aldrich, USA), 50 µM α-synuclein and 1.5 µM nanoparticle in MilliQ. The same nanoparticles are used in the ThT assay as in the MST. Next to that, the unlabelled variant of the nanoparticles is used. The amount of tertiary amine in these particles is the same as in the labelled nanoparticles. The six nanoparticles and the control (without nanoparticles) are added in triplicates in a black half area 96-wells plate with clear bottom (Corning, USA). The fluorescence is measured over time in a plate reader (Infinite 200 Pro, Tecan Ltd., Switzerland) at 37°C with an excitation wavelength of 446 nm, the fluorescence is measured at 485 nm. 5300 cycles are measured, each cycle consists of 10 minutes of orbital shaking with an amplitude of 1.5 nm and a fluorescence measurement in five flashes, integrated over 20 µs with a gain of 80. This means the aggregation will be measured over more than a month.

The fluorescence intensity is averaged via a moving average over 20 points, all curves are then normalized. The lag time is estimated as the point where the fluorescence value has increased to four times its initial value, given that the aggregation keeps increasing from that point on.

2.5 Cell culture

The culture medium consists of DMEM/F-12 (Gibco, Invitrogen, USA) with 10% heat inactivated FBS (Gibco, Invitrogen, USA), 1% Penicillin/Streptomycin (Gibco, Invitrogen, USA), 1% non-essential amino acids (Gibco, Invitrogen, USA), and 10 mM HEPES (Gibco, Invitrogen, USA). The cells used are SH-SY5Y cells (ATCC, USA), both unmodified and after transfection. For the transfection a plasmid is added creating an overproduction of α-synuclein with a FLAG-tag. The two cell lines will be called 'normal' and 'FLAG' in this research. For the uptake and aggregation analysis, cells are seeded in an ibidi microslide, coated with collagen IV (µ-Slide VI 0.4, ibidi GmbH, Germany). For the viability analysis, cells are seeded in a black tissue culture treated 96-wells plate (Greiner Bio-One, Austria). The cells are seeded when they reach full confluency in the culture flask.

2.6 Adding nanoparticles and WGA-staining

To determine the uptake of particles in endosomes or the cytosol, wheat germ agglutinin (WGA) can be used. This protein binds to the glycoproteins of the cell membrane, more specifically to N-acetyl glucosamine and N-acetyl neuraminic acid residues oligosaccharides [26, 27]. WGA can also be used to stain the Golgi apparatus and some vesicles [28]. P. Ramoino et al. visualised the internalisation of WGA and found that it is visible in endosomes [29]. This shows that WGA can be used to follow the internalisation process.

A solution is made of 1% FBS medium (DMEM/F12, 1% heat inactivated FBS, 1% Penicillin/Streptomycin, 1% non-essential amino acids, and 10 mM HEPES) with 250 nM nanoparticles. The solution is added 24

hours after seeding the cells. 24 hours after adding the nanoparticles, the cells are washed two times with PBS (Gibco, Thermo Fisher Scientific, USA) and then fixed in PBS with 3.7% PFA (Merck, Germany) for 15 minutes at room temperature. The cells are washed three times with PBS and the Wheat Germ Agglutinin in a concentration of 5.0 µg/mL (Invitrogen, Thermo Fisher Scientific, USA) is added.

The cells are imaged using the MicroTime 200 in PIE mode (20 MHz frequency) with excitation wavelengths of 640 and 485 nm. The intensity is measured at a wavelength of 670-710 nm and 485-555 nm. The images are analysed using a Python script, which colours each channel a specific colour and changes the brightness upon signal intensity. The intensity is normalised to the highest intensity of the specific channel. To analyse whether the green fluorescent signal is from autofluorescence of the cell or from the nanoparticles, the lifetime is analysed. This is done using FLIM analysis in SymPhoTime 64. A shorter lifetime is given a different colour than a longer lifetime, where a short lifetime points to autofluorescence [30, 31].

2.7 Nanoparticle uptake and α-synuclein staining

For the uptake, nanoparticles are added in a concentration of 1250 nM in medium with 1% FBS. After 72 hours, the cells are fixated and the α-synuclein is stained. For that, the cells are first fixated following the protocol of the WGA-staining, except the step where the WGA is added. After washing the cells three times with PBS, the cells are permeabilised in PBS with 0.3% saponin (Fluka, Sigma-Aldrich, USA) and 0.1 % bovine serum albumin (BSA, Sigma-Aldrich, USA) for 30 minutes at room temperature. The cells are then washed with PBS again. The autofluorescent signals are quenched with 50 mM NH_4Cl (Merck, USA) in PBS for 15 minutes at room temperature. Aspecific sites are blocked with goat serum dilution buffer (GSDB) for one hour at room temperature, GSDB consists of PBS with 16% goat serum (Merck, USA), 0.3% saponin, and 0.3 M NaCl. The cells are incubated for an hour at room temperature with anti FLAG (diluted 1:1000 in GSDB, Sigma-Aldrich, USA) or anti α-synuclein (diluted 1:2000 in GSDB, BD Transduction Laboratories, USA). The cells are washed three times with PBS with 0.3% saponin and 1% BSA and after that incubated for 30 minutes with anti mouse (Invitrogen, USA), diluted 1:200 in 0.3% saponin and 0.1% BSA in PBS. The cells are washed twice with 0.3% saponin and 0.1% BSA in PBS for five minutes. The fixed cells are then incubated with DAPI (Invitrogen, USA), diluted 1:500 in PBS, for 15 minutes and washed four times with PBS after.

Imaging of the cells is equal to the imaging of the WGA-staining.

2.8 Electroporation and α-synuclein staining

The technique electroporation is based on the usage of electricity to create pores in the cell. Via those pores, plasmids or nanoparticles can enter the cytosol. The transient aqueous pore theory is the most used model to explain electroporation. Due to the electric field, hydrophilic pores can grow out of hydrophobic defects. The shrinking of pores happens rapidly when the electric field is turned off, it does however take seconds to minutes before the pores are fully closed [32].

The electroporation is done using the 4D-Nucleofector X Unit (Lonza, Switzerland) and a protocol for this machine and the SH-SY5Y cells [33], together with the recommended V4XC-2012 kit (Lonza, Switzerland). For this experiment, the FLAG cell line is used, with $1 \cdot 10^5$ cells per cuvette. There are 6 conditions: three types of nanoparticle (0%, 30% and 60% tertairy amine) and three controls. Nanoparticles are added in a concentration of 250 nM. The controls consist of a control for effect of the nucleofection program on the cells (nothing added), a control for the nucleofection itself (using the GFP vector in the kit) and a control for the possible toxicity of Tris, in which the nanoparticles are diluted. After the nucleofection, cells are seeded in 8-well chambers, coated with Collagen IV (ibidi GmbH, Germany) in a seeding density of $1 \cdot 10^5$ cells/cm^2. In this case, 10% FBS medium is used. Every condition is plated in duplicates. The cells are stained after 24 hours, where the protocol is similar to the protocol used for the uptake.

The imaging is equal to the imaging used above. To determine the electroporation efficiency, 5 images per duplicate are made of the GFP control. The percentage of cells expressing GFP is the transfection efficiency. Next to that, the amount of α-synuclein clusters in 40 cells per sample is counted.

2.9 Cell toxicity

To determine the effect of certain components on the cells, the viability needs to be assessed. The metabolic activity is an important measure of the cell's viability [34]. To assess this, resazurin is used commonly. Resazurin is a weak fluorophore which gets reduced in the cell to resorufin by NAD(P)H-dependent oxidoreductases and dehydrogenases. Resorufin is strongly fluorescent, with an excitation wavelength of 570 nm and an emission wavelength of 585 nm. The assay gives insight into the metabolism of the cell. A higher fluorescent signal means more resorufin is produced and the cell has a higher metabolic activity [35, 34]. As mentioned before, α-synuclein aggregation can also affect the mitochondria, this creates an increase in the amount of reactive oxygen species (ROS) [7]. These ROS are produced as a byproduct of the aerobic respiration, functioning in cell signaling. In a high amount they are associated with oxidative stress [36]. DCFH-DA (2',7'-dichlorofluorescin diacetate) is used to assess the amount of ROS. DCFH-DA can diffuse into the cell, where esterases hydrolyze it to DCFH (2',7'-dichlorofluorescin). DCFH is polar and stays in the cell, if there's ROS present DCFH gets oxidized to the fluorescent molecule DCF (2',7'-dichlorofluorescein) [37]. DCF has an excitation wavelength of 488 nm and an emission wavelength of 525 nm [38].

To assess the metabolic activity, the CellTiter-Blue viability assay (Promega, USA) is used. For the amount of ROS the fluorimetric intracellular reactive oxygen species assay (Sigma-Aldrich, USA) is utilized. Both tests are done in a 96-wells plate in triplicates. The FLAG and normal cell lines are also used here and seeded in a seeding density of 20,000 cells/well. One day after seeding the nanoparticles are added in a concentration of 250 nM in 1% FBS medium. After 3 days the medium with nanoparticles is replaced for the 1% FBS medium without nanoparticles. 6 days after seeding both tests are executed according to the manufacturer's protocol. All conditions are measured in triplicates, the positive control consists of the cells that are not treated with nanoparticles. The negative control is an empty well, with only the solution of the kits added. The fluorescence is measured in the plate reader with an excitation/emission wavelength of 560/590 nm for the CellTiter-Blue assay and 540/570 nm for the reactive oxygen species assay, as stated in the corresponding protocols. The negative control is subtracted from all data, as this is the background signal. The positive control is used to normalise the data.

3 Results

3.1 Fluoroscence correlation spectroscopy

Nanoparticles in the cell can cluster if they are bound to the membrane, but they can also enter the cell already clustered. With fluorescence correlation spectroscopy (FCS) the hydrodynamic size is determined to see if the nanoparticles are clustered. The size is also relevant for the uptake by the cell. Next to that, the lifetime can be found as a way to find possible abnormalities in the nanoparticles.

The TCSPC data shows that the 0% and 60% have a comparable lifetime, where the lifetime of the 30% is shorter (Table 1). To possibly fix this, the nanoparticle with 45% tertiary amine was also tested. The TCSPC graphs are shown in Figure 1. The 45% nanoparticle has a higher intensity than the other nanoparticles. This nanoparticle also has a much shorter lifetime, as can be seen in Figure 1 and in the τ-value in Table 1. The 45% nanoparticle is therefore not considered further in this research.

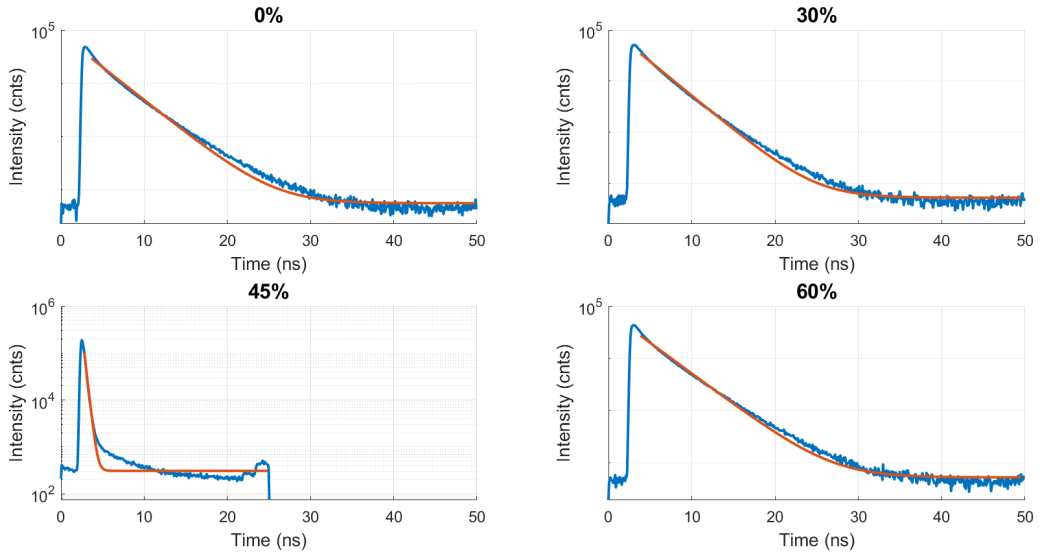

Figure 1: The TCSPC graphs of the different nanoparticles. The red line shows the fit of the data (blue).

Table 1: The lifetime, following Formula 2, of the different nanoparticles diluted in MilliQ.

	0%	30%	45%	60%
τ(ns)	3.35 $\pm$ 0.03	3.14 $\pm$ 0.03	0.33 $\pm$ 0.01	3.55 $\pm$ 0.04

MilliQ is the initial solvent of the nanoparticles, but when the nanoparticles come into contact with the cell they are put in cell culture medium. This can possibly cause nanoparticle aggregation. The hydrodynamic size of the nanoparticles is measured again after six days to find out if there was an equilibrium in the earlier measurement. The autocorrelation curves of the different nanoparticles are shown in Figure 2. For the 0% and 30% nanoparticle, the curve shifts to the right when the nanoparticles go from MilliQ to medium. The 30% nanoparticles in MilliQ display a curve shaped different than the other curves. All correlation curves shift to the left once they are in the cell culture medium for multiple days (Figure 2). A curve shifting to the right means the diffusion speed decreases. According to Formula 1 the hydrodynamic radius increases with a decreasing diffusion speed. The shift the curves in Figure 2 make is however not big enough to state that the radius in the nanoparticles differs, calculations are needed for that.

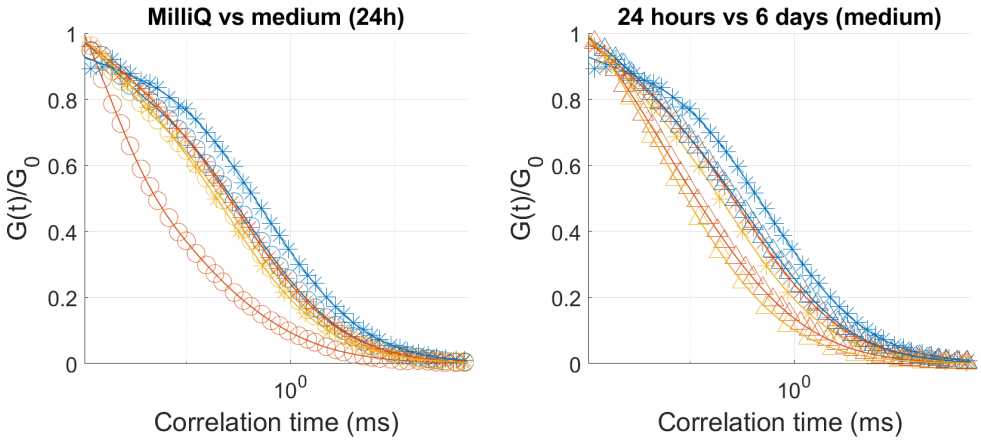

Figure 2: The FCS autocorrelation curves, normalized to $G(t_0)$. The markers show the $G(t)/G_0$ for the nanoparticles in MilliQ (circles), 24 hours in medium (stars) and 6 days in medium (triangles). The fit is shown as a line through the markers. The different colours represent the nanoparticles with 0% (blue), 30% (red) and 60% (yellow) tertiary amine. The curves are averaged over the eight measurements done per sample. For clarity of the graph, not all points are displayed.

The diffusion speed of the different nanoparticles is given in Table 2. The hydrodynamic radius of the nanoparticles is calculated using Formula 1 and given in Table 2 as well. In MilliQ, the nanoparticles are around 12 nm (Table 2). The mean hydrodynamic radius increases if there is a significant number of aggregates. After 24 hours in 1% FBS medium the hydrodynamic radius of the 0% nanoparticle is barely affected, the hydrodynamic radii of the 30% and 60% nanoparticle do however roughly triple. In both cases, the error also increases significantly. Due to the variance some nanoparticles will be unable to enter the cell, while others have no problem entering the cell. After 6 days, the 30% and 60% nanoparticle do not aggregate more. The hydrodynamic radius of the 0% nanoparticles does increase after 6 days in 1% FBS medium, where it did not change after 24 hours. The radius doubles compared to the earlier measurements.

Nanoparticles in medium thus have a higher hydrodynamic radius due to aggregation. The 30% and 60% nanoparticle are earlier affected by this than the 0% nanoparticle (Table 2). A longer time in the 1% FBS medium does not lead to a bigger hydrodynamic radius for the positively charged nanoparticles.

Table 2: The diffusion speed and hydrodynamic radius of the different nanoparticles, calculated using FCS. The nanoparticles are left in the 1% FBS medium for 24 hours at -4˚C and the subsequent five days at 21˚C.

		Diffusion speed ($\mu m^2/s$)	Hydrodynamic radius (nm)
In MilliQ	0%	17.1 ± 0.2	12.7 ± 0.2
	30%	26.0 ± 0.9	9.3 ± 0.4
	60%	19.8 ± 0.7	14 ± 1
In 1% FBS medium (24 hours)	0%	17.7 ± 0.5	14.1 ± 0.7
	30%	12.1 ± 0.7	28 ± 4
	60%	11 ± 1	41 ± 8
In 1% FBS medium (6 days)	0%	8.6 ± 0.4	26 ± 1
	30%	8 ± 1	30 ± 6
	60%	10 ± 1	36 ± 10

3.2 Microscale thermoporesis

Microscale thermoporesis (MST) is done to determine the binding affinity of the nanoparticles to α-synuclein. This is the first step in the aggregation process. The binding curves of the MST are given in Figure 3. If one concentration is laying above the fit in all three curves, it is taken as an outlier. These are also shown.

The curves after 30 minutes of incubation are shown, as there was an equilibrium at that point in time. The binding curve shifts to the left with more tertiary amine in the nanopolymer.

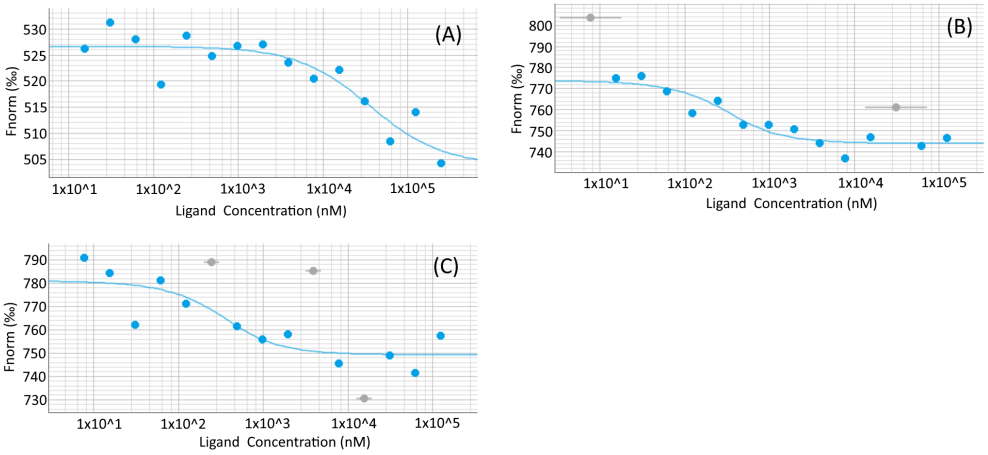

Figure 3: The binding curves, following the K_D-model, of the nanoparticles with (A) 0% tertiary amine, (B) 30% tertiary amine and (C) 60% tertiary amine, measured with MST. Only the curve at 80% MST power is displayed. The grey points are assumed to be outliers and not taken into account with the fit.

The binding constant K_D is given in Table 3, it can be seen that K_D decreases with increasing nanoparticle charge. This means that the binding is stronger with a higher percentage of tertiary amine in the nanoparticle, which can also be seen as a higher charge. The confidence interval is broad. In the case of the 60% nanoparticle, the confidence interval is greater that the value itself (Table 3). The trend between the values is however more important, it being that the binding is stronger in nanoparticles with a higher charge.

Table 3: The binding constant K_D of the different nanoparticles to α-synuclein, including the 68% confidence interval. The K_D is calculated as the mean of the three binding constants found from the different MST powers (20%, 40% and 80%).

	K_D (nM)
0%	$6.24 \cdot 10^5 \pm 2.74 \cdot 10^5$
30%	555±385
60%	201±257

3.3 ThT aggregation assay

The ThT assay gives insight in the lag time of α-synuclein in combination with the nanoparticles. The lag time shows if the nanoparticles speed up aggregation. The result from the ThT assay is shown in Figure 4. To check if the labelling has an effect on the aggregation, the aggregation induced by unlabelled nanoparticles is shown in Figure 5. One of the triplicates of α-synuclein spontaneously aggregated after around 100 hours, this measurement is taken as an outlier and not included in the data as it differs strongly from the other two samples. For the labelled 30% nanoparticle, one of the triplicates shows seemingly random peaks and drops, and is therefore considered as an outlier.

The nanoparticles with 0% tertiary amine show aggregation after more than 500 hours in the labelled variant (Figure 4). The unlabelled particle induces aggregation a bit later, the aggregation is also quite noisy. In the 30% nanoparticle, aggregation is seen in both variants, both graphs show a sigmoidal curve. The labelled 30% nanoparticle shows a bump at 300 hours, this bump is also seen in the other graphs. This bump is assumed to be an instrumental error and mostly interferes with the graph for the labelled 30% nanoparticle. In the labelled 60% particle, there are multiple plateaus. Only the first plateau is displayed in Figure 4. In

the unlabelled 60% nanoparticle, the ThT fluorescence decreases after it reached its maximum value. This is cut off in Figure 5, it can however also be seen by the other nanoparticles in Figure 4 and Figure 5.

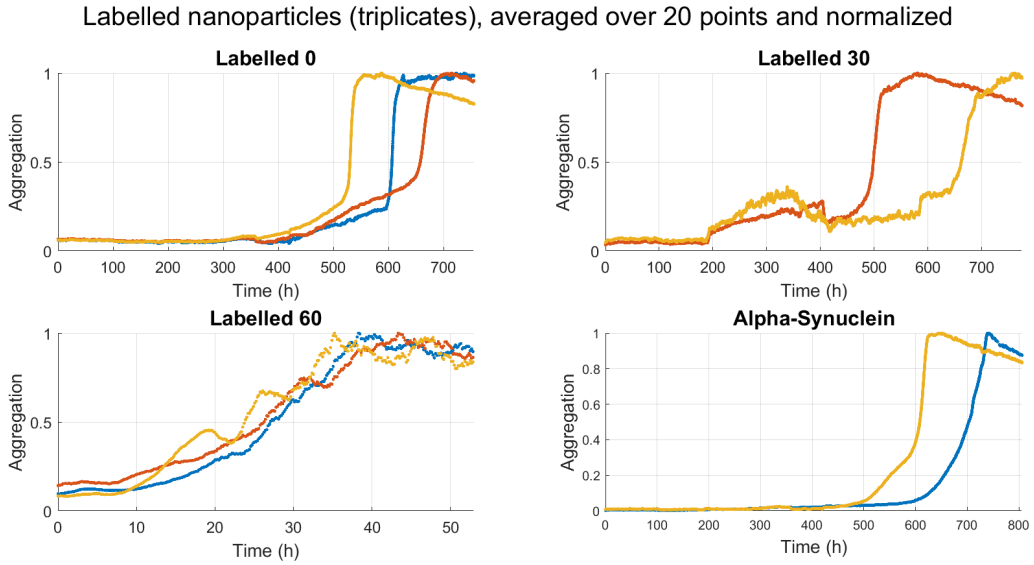

Figure 4: Normalized data of a-synuclein aggregation, induced by nanoparticles with a different percentage of tertiary amine. The graphs are cut off at the first plateau.

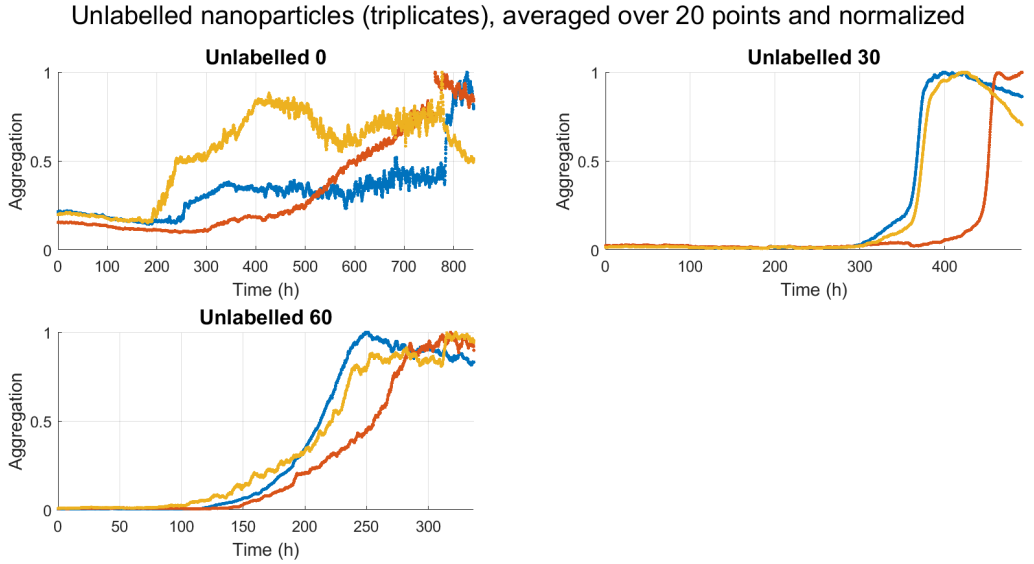

Figure 5: Normalised data of a-synuclein aggregation, induced by nanoparticles with a different percentage of tertiary amine. This figure shows the unlabelled nanoparticles, to show if the labelling has an effect on the aggregation. The graphs are cut off at the first plateau

The lag time is shown in Table 4. There is a difference between the labelled and unlabelled variant. It can however be seen that the higher the percentage of tertiary amine, the shorter the lag time. This happens in both cases, both the unlabelled and the labelled nanoparticles follow a comparable trend. As can be seen in

the graphs, the lag time varies per sample (Figure 4 and Figure 5). This effect is seen in the high standard deviation of some samples (Table 4). A-synuclein has an average lag time of 374 ± 138 (SD) hours. This is less than the lag time of both the labelled and unlabelled 0% nanoparticle (Table 4). The lag time of the labelled 30% nanoparticle is also longer than the lag time of α-synuclein, the unlabelled 30% nanoparticle has a bit shorter lag time than α-synuclein. The bar graph (Figure 6) shows a decrease in lag time if the amount of tertiary amine increases. This means that a higher charge results in faster aggregation. When the error is taken into account, the lag time between the labelled and unlabelled particle is comparable, except for the 60% nanoparticle (Figure 6).

Table 4: The lag time (hours) of aggregation of α-synuclein induced by different nanoparticles. The lag time is determined as the value where the fluorescence intensity reaches four times its initial value, except for the labelled 30% nanoparticle as this graph is greatly influenced by an instrumental error.

	Labelled	Unlabelled
0%	547 ± 49 (SD)	619 ± 206 (SD)
30%	452 ± 139 (SD)	355 ± 58 (SD)
60%	22.6 ± 6.6 (SD)	127 ± 22 (SD)

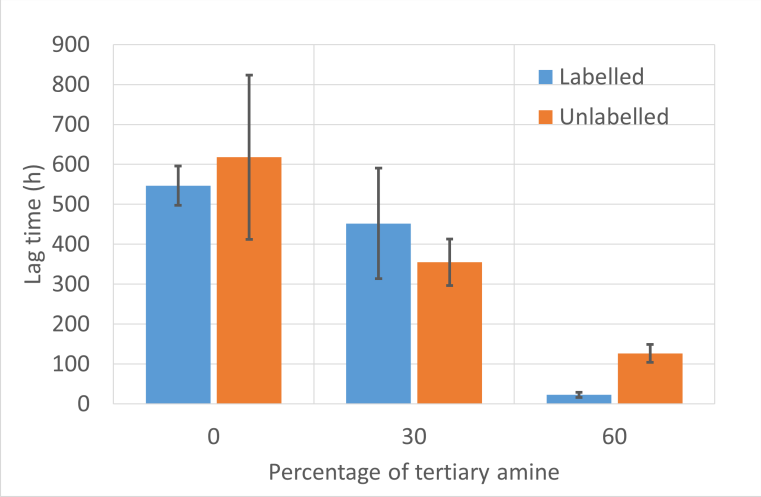

Figure 6: The lag time including the error, as given in Table 4. The lag time is given as four times the initial fluorescence value of ThT assay, except for the labelled 30% nanoparticle as this graph is greatly influenced by an instrumental error. The errorbar shows the standard deviation.

3.4 Nanoparticle uptake

To determine if the nanoparticles are taken up and in the cytosol, the cell membrane is stained using a WGA-staining.

The result of the WGA-staining is given in Figure 7. It can be seen that the nanoparticles give off a much brighter signal in the 60%, there were however no abnormalities reported from the preparation of the solution. Clusters of nanoparticles can be seen as small dots in the cells. There is no visible WGA-stain around any of the nanoparticles, apart from the expected cell membrane.

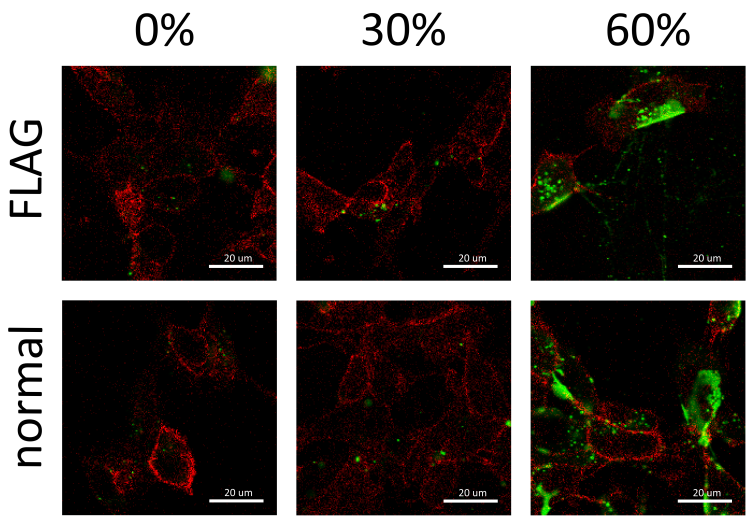

Figure 7: The result of the WGA-staining with a magnification of 60x. The cells are fixed 24 hours after adding the nanoparticles in a concentration of 250 nM. The red signal shows the membrane, stained with WGA. The green signal shows the nanoparticles.

By processing the images on a logarithmic scale, the nanoparticles are not only visible as clusters. The logarithmic scale makes the different intensities lay closer to each other, this does mean that autofluorescence can be seen and that noise has a bigger effect. In Figure 8 it can be seen that there is a strong diffuse signal in the cells with the 60% nanoparticle. In the FLAG cell line some background signal can be seen in the sample with the 60% nanoparticle. For the 0% and 30% nanoparticle, the green signal is more 'grain'-like. In the normal cell line, there is also diffuse signal seen with the 30% nanoparticle. It is hard to see the diffuse signal under the grain-like signal, making it difficult to see if there is any diffuse signal at all in the cells with 0% and 30% nanoparticles. The difference between the cell lines is not noticeable.

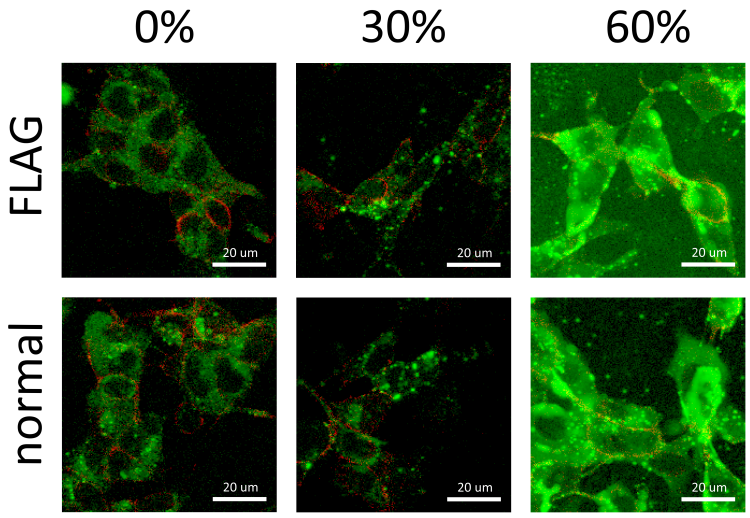

Figure 8: SH-SY5Y cells after 24 hour incubation with 250 nM green fluorescent nanoparticles, stained with a WGA and imaged with the MicroTime 200 (60x). The images are processed by putting the signal on a logarithmic scale. The red colour shows the membrane, stained with WGA. The green colour shows the nanoparticles.

Figure 8 shows grainy, but also diffuse green fluorescent signals. To determine the source of this signals, the lifetime is analysed (Figure 9). The intensity is normalised, for the 0% and 30% this does not change a lot but the initial intensity of the 60% nanoparticle is roughly 10 times higher. The grainy signal is seen in the cells with 0% and 30% tertiary amine nanoparticles (Figure 8). The cells with the nanoparticles with 0% tertiary amine show quite some red signal. The signal is however not as diffuse as in the 60%, it is grain-like as mentioned before. In the cells with the 30% nanoparticles, there are more parts with a short lifetime (Figure 9). The cells with the 60% nanoparticles have quite some signals with a lifetime close to 3 ns. The bright signals as seen in Figure 7 have a very short lifetime (Figure 9). The 30% nanoparticles show a relatively short lifetime, as there is not a lot of red seen in the figure. The 0% and 60% nanoparticle show more red signal, where the intensity in the 60% nanoparticle is significantly higher.

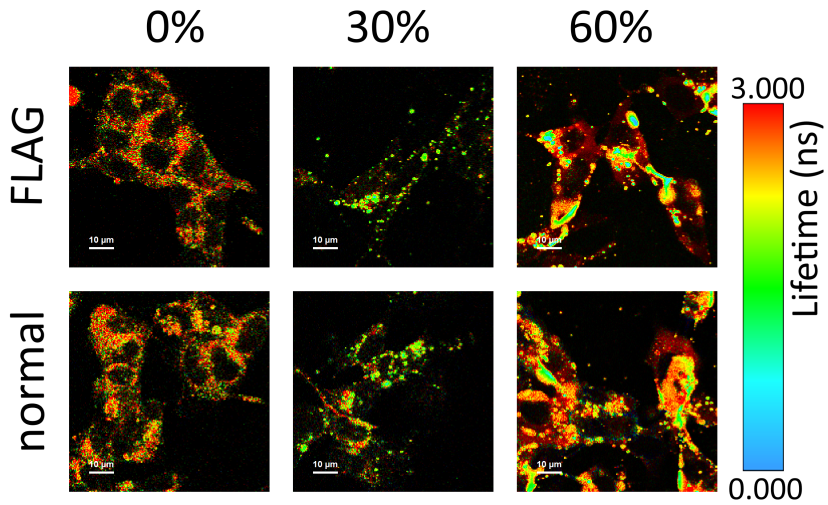

Figure 9: The lifetime of the signals measured at 485-555 nm, showing 250 nM nanoparticles added to SH-SY5Y cells 24 hours prior to imaging.

3.5 Effect of nanoparticles on α-synuclein in the cell

The effect of the nanoparticles of α-synuclein in the cell is determined using an α-synuclein staining. Nanoparticles are added to the cell in two different ways: by cellular uptake and by electroporation. With electroporation, the clustering of nanoparticles due to the cell culture medium is prevented.

3.5.1 Nanoparticle uptake

In Figure 10 it is clear that the FLAG cell line produces more α-synuclein than the normal cell line. There is no green fluorescent signal in the control, where no nanoparticles are added. The trend in the amount of particles is similar to the WGA-staining. The green fluorescent spots coming from the 60% nanoparticle are not as bright, but still more apparent than the 0% and 30% nanoparticle. In the FLAG cell line, there are some brighter spots of α-synuclein seen with the 30% and 60% nanoparticle. The spots do seem close to the nanoparticles, but don't occur in all cells with nanoparticles. There are also vague spots seen in the control group from the FLAG cell line, the 60% nanoparticle does however have noticeably more α-synuclein dots (Figure 10). In the normal cell line, no dots are seen.

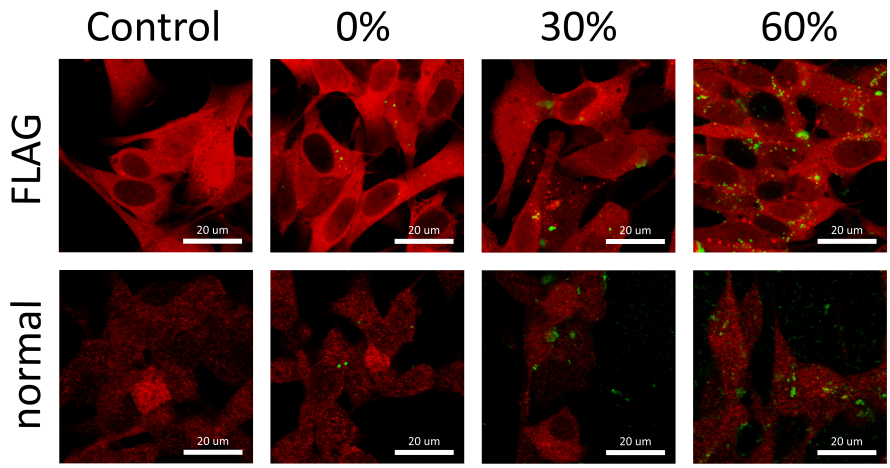

Figure 10: 1250 nM of nanoparticles added to SH-SY5Y cells, where the a-synuclein production is enhanced in the FLAG cell line. The images are made at a magnification of 60x, 72 hours after adding the nanoparticles. The red colour shows a-synuclein, the nanoparticles are shown in green.

3.5.2 Electroporation

The electroporation efficiency is 45 ± 9 (SD) percent, determined from counting 130 cells in the GFP control. Due to the electroporation, the nanoparticles should be in the cytosol. This creates such a diffuse light that it is barely distinguished from autofluorescence. The difference between the Tris and the protocol control is not visible, meaning Tris does not have an effect on the cells. The images are shown in Figure 11. There are less clusters of nanoparticles in Figure 11 than in Figure 10, the clusters are also smaller.

Clusters of α-synuclein can be seen as bright red spots in the cells. These spots are also seen in the control, where no nanoparticles are added. The clusters appear with a size of 500 nm, which is close to the diffraction limit of the microscope (270 nm). In the cells with the nanoparticle with 0% tertiary amine, some small clusters can be seen, especially at the bottom left. The cells with the 30% nanoparticles have more clusters than in the cells with the 0% nanoparticles (5.5 ± 7.9 (SD) α-synuclein clusters per cell in the 30% versus 4.9 ± 4.3 (SD) in the 0%). The 60% has roughly the same amount of clusters per cell as the 30% (5.4 ± 4.3 (SD) clusters per cell). Some α-synuclein clusters in the cells with the 60% nanoparticle are bigger, around 2 µm. The cells with GFP have the highest amount of clusters, namely 7.5 ± 7.3 clusters per cell. The amount of clusters is however not significantly bigger than in the controls (3.4 ± 7.7 (SD) α-synuclein clusters per cell). Next to that, the standard deviations are high, showing that the amount does not significantly differ between the different conditions.

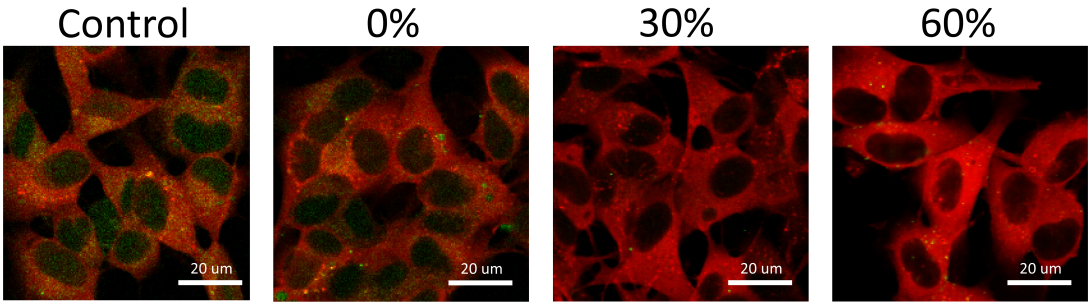

Figure 11: FLAG SH-SY5Y cells 24 hours after electroporation with 250 nM nanoparticles. The a-synuclein is stained and cells are imaged using a fluorescence confocal microscope at a magnification of 60x. The red colour shows a-synuclein, the nanoparticles are shown in green.

3.6 Cell toxicity

To determine the effect of the nanoparticles on the viability of the cell, the metabolic activity is measured. The amount of reactive oxygen species gives insight in the health of the mitochondria. In all cell toxicity data, the row on the side of the 96-wells plate has much lower values compared to the rest. These values are therefore taken out, leaving the experiment in duplicates. The results of the metabolic assay and the reactive oxygen species assay are shown in Figure 12.

The metabolic activity decreases with an increasing nanoparticle charge. The metabolism of the FLAG cell line decreases more than the metabolism of the normal cell line with an increasing percentage of tertiary amine in the nanoparticles. For the 30% nanoparticle, the FLAG cell line has a big error in metabolic activity. Remarkable is the relatively low metabolic activity of the control group compared to the cells with the 0% nanoparticles and the normal cell line with the 30% nanoparticle.

The reactive oxygen species varies less than the metabolic activity. In the normal cell line the amount of ROS (reactive oxygen species) is lower in the samples with 0% and 30% nanoparticles than in the control group. The amount of ROS is higher in the cells with the 60% nanoparticle than in the cells with the 30% and 0% nanoparticle, meaning there is more oxidative stress. In the normal cell line, the amount of ROS for cells with the 30% nanoparticle is also higher than for cells with the 0% nanoparticle, for the FLAG cell line this is the other way around.

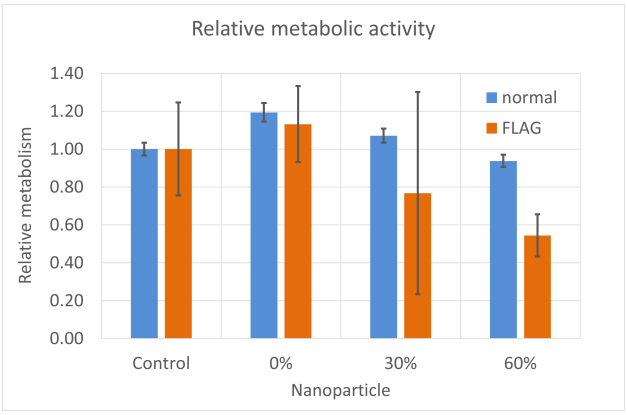

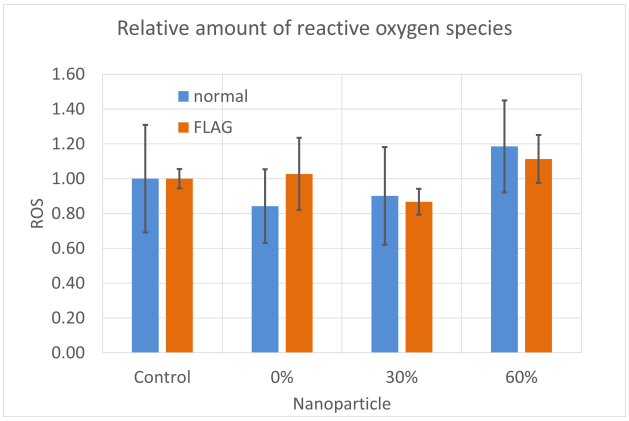

Figure 12: Two types of cell toxicity assays, normalised to the untreated control. Two cell lines are used: normal and FLAG. Nanoparticles are added 1 day after seeding in a concentration of 250 nM. 5 days after adding the nanoparticles the metabolic activity of the samples is assessed, as well as the relative amount of reactive oxygen species. The standard deviation is given as an error bar.

The amount of resorufin produced and thus the fluorescence intensity is dependent on the amount cells. More cells also increase the amount of ROS in the sample and thus lead to an invalid comparison between samples as each sample can have a different amount of cells. The cells are seeded at the same density, but over time error in this can increase greatly as the cells grow at a different rate depending on the confluency. Both cell lines show a high metabolic rate in the samples with the 0% nanoparticle (Figure 12). Assuming that all cells have the same metabolic rate and thus assuming that the amount of resorufin produced is only dependent on the amount of cells, makes it possible to correct the amount of ROS for the amount of cells. This leads to an increasing amount of ROS for both cell lines with increasing nanoparticle charge (Figure 13). This result is however based strongly on the assumption that the metabolism for the total sample is only dependent on the amount of cells.

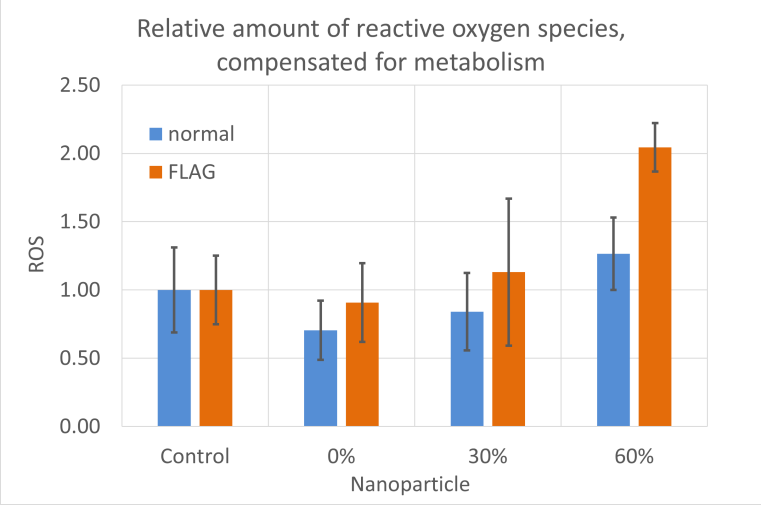

Figure 13: The relative amount of reactive oxygen species in two cell lines 24 hours after adding different nanoparticles (250 nM). The amount of ROS is compensated by the metabolic activity of the sample as a whole, assuming the resorufin production is only dependent on the amount of cells. The standard deviation is given as an error bar.

4 Discussion

4.1 Nanoparticle characterisation (FCS)

With the FCS measurement it was found that the hydrodynamic radius increases in the cell culture medium, as a consequence of nanoparticle aggregation. The cause for this will be discussed. Next to that, there will be paid attention to the short lifetime of the 45% nanoparticle and the divergent autocorrelation curve of the 30% nanoparticle. Lastly, the effect of nanoparticle aggregation on cellular uptake will be discussed.

First thing standing out was the short lifetime of the nanoparticles with 45% tertiary amine. The lifetime of fluorophores can decrease by temperature, polarity and quenching [39]. Quenching happens due to molecular interactions [40]. Molecules can also self-quench when the concentration of fluorophores is high, which can happen because of aggregation or over-labelling [41]. The most plausible cause for the short lifetime of the 45% nanoparticle is over-labelling, this is however not reported in the research from N.M. Hamelmann et al. [14].

Figure 2 shows an abnormal curve of the 30% nanoparticle in MilliQ. The triplet state has a lifetime in the nanoseconds to milliseconds, with green fluorescent particles even having a triplet state lifetime of around 5 ms [42]. Looking at the figure, this can interfere with the nanoparticle correlation time. Next to that, the graphs are normalised, meaning that the normalisation can make it seem like the starting plateau for the fluorophore diffusion time is at the same level as the plateau for the triplet state. It is recommended to normalise the graph according to the first plateau after the triplet state, leaving only the diffusion of the complete molecule in the graph.

As seen in Table 2, the medium induces some degree of aggregation. The ion concentration and the pH-level impact the stability of collisions, meaning these factors influence if collisions form aggregates or fall apart. Proteins like FBS also interact with nanoparticles and can either stabilise or destabilise them, leading to possible aggregation [43]. K. Rausch et al. showed that gold nanoparticles aggregate when they are in human plasma [44]. Human plasma does however have a much more proteins than medium with FBS [43]. The proteins in the cell culture medium are probably the cause for the aggregation of the nanoparticles.

The radius does increase once the nanoparticles form clusters. The size of a nanoparticle is a factor in the cellular uptake, making it relevant to determine this. The optimal size for uptake is 50 nm, nanoparticles smaller than 15 nm are however not considered in the research determining that optimum [45]. Smaller nanoparticles are taken up quickly [46]. The aggregates do not exceed the optimum, meaning they are probably taken up well. From this it can be concluded that although the particles increase in size by aggregation, the aggregation does not influence the uptake. The difference between individual measurements increases as possible aggregates will be of different sizes or not appearing in all measurements, some particle aggregates can be too big to be taken up while others are still small and their uptake is not limited by size. The surface to volume ratio does however decrease, making the nanoparticles less reactive as some reactive sites are inside the cluster [46].

4.2 Aggregation assay and binding affinity

With the MST it is seen that the K_D value decreases with an increasing amount of tertiary amine, the found K_D values will be compared to the binding affinity of antibodies for more context. With the ThT aggregation assay, it is found that the lag time decreases for an increasing tertiary amine percentage. The lag time of α-synuclein aggregation will be compared to other research, as well as the cause of a decreasing fluorescence value after the aggregation reaches the plateau. Lastly, the relevance of the lag time for this research will be discussed, considering the incubation time of the nanoparticles with the cells.

To put the K_D values in perspective, the binding constant is compared to antibodies. Antibodies are considered to have a high binding affinity when the K_D is smaller than 10^{-10} M and a low binding affinity when the K_D is above 10^{-6} M. Everything in between that is considered a medium binding affinity [47]. With a K_D of $6 \cdot 10^{-4}$ M, the nanoparticle with 0% tertiary amine can be placed in the low binding category. The 30% and 60% nanoparticle have a medium binding affinity, considering the antibody categories. This is not unexpected, as the 0% nanoparticle is the only negatively charged nanoparticle and α-synuclein is also negatively charged [6]. The standard deviation of the binding affinity measured with MST is high, but does not interfere with the results. The trend of a higher binding affinity for a higher percentage of tertiary amine

in the nanoparticles is still visible.

Other researchers find a lag time of less than 100 hours [13, 48, 49]. This is a lot faster than the lag time for α-synuclein aggregation found in this research. Even the control, α-synuclein without nanoparticles, shows a lag time of almost 400 hours. In other research a lag time of less than 24 hours is found [50, 51]. There is thus aggregation, but it takes long to form. The aggregation of α-synuclein in the control is happening before the aggregation with the 0% nanoparticle, this leads to the believe that the α-synuclein aggregation is not induced by the 0% nanoparticle. That correlates with the research from M. Mahmoudi et al., they found that small negatively charged nanoparticles inhibit aggregation [3]. For the 30% nanoparticle, it is questionable if it speeds up aggregation or not, as the lag time is very close to the lag time of α-synuclein. The 30% nanoparticle might speed up aggregation a bit, but not as extensive as the 60%. The 60% nanoparticle does induce aggregation quite fast.

Most of the nanoparticles show a decrease in ThT fluorescence after the plateau, this can possibly be caused by evaporation or by photobleaching. If the solvent evaporates, the liquid level decreases. This can lead to the focus point being partly above the sample and thus measuring less sample. There is no ThT and therefore no fluorescence above the sample, meaning the fluorescence value decreases as the solvent slowly evaporates. This is, just like photobleaching, a speculation. The exact cause of the decrease in fluorescence intensity is not known. To rule the effect of evaporation out, more sample can be added to the wells. Adding solvent in between the wells is also an option, this is already done in this research.

In other experiments in this research, cells are incubated with the nanoparticles for maximum 72 hours (except for the toxicity), this means that the lag time for the 0% and 30% won't be reached. It is questionable if there will be any visible aggregation if the incubation time is not long enough.

4.3 Nanoparticle uptake

The WGA-staining is used in this research to envision the uptake mechanism of the nanoparticles. This data is compared to research in which the same nanoparticles are used. Next to that, the way WGA stains the cells is analysed further to clarify the results found. Lastly, the lifetime of the nanoparticle images is discussed. The effect of autofluorescence and quenching on the image processing is considered.

N.M. Hamelmann et al. found that the 0% nanoparticles are encapsulated in a vesicle to later fuse with a lysosome. The 30% nanoparticles taken up less and partly fused with lysosomes. In their research, the 60% nanoparticle was free in the cytosol [14]. From the WGA-staining it is clear that the 30% nanoparticle is indeed internalised less, as there is not a lot of signal. The 60% nanoparticle does show a diffuse signal, meaning it's partly in the cytosol. N.M. Hamelmann et al. also saw some clusters, but not to the same extent as in Figure 7. The 0% nanoparticle shows some uptake, the images are similar to the research from N.M. Hamelmann et al. [14].

The absence of a plasma membrane around the 0% and 30% nanoparticles is not correlating with the data from N.M. Hamelmann et al., as they show (partly) colocalisation with lysosomes [14]. Wheat Germ Agglutinin stains all digestive membranes and thus should also stain the endosomes [52]. The WGA-stain must however go into the cell to do this and the substance itself cannot go through the cell membrane. The cells are only fixed and not permeabilised, using permeabilization will allow the WGA to cross the membrane and stain the intracellular vesicles. A problem in this is however that the organelles can also be stained, making it hard to distinguish different structures. A different staining, like a lysosomal staining, might be more beneficial to determine the uptake mechanism of nanoparticles.

Autofluorescence is caused by for example aromatic amino acids and NADPH/NADH [53]. As measured with the FCS, the lifetime of the nanoparticles is 3 to 3.5 ns, but can be way shorter once they are quenched. The quenching can, next to over-labelling, also happen because of big nanoparticle clusters. These big nanoparticle cluster are seen in the WGA-stained cells with the 60% nanoparticles. The lifetime of NADH, is below 2.5 ns [31], making it possible to distinguish the two signals if quenching was not happening. Quenching makes the lifetime of the nanoparticles and the cell components come closer together, leaving a colourful lifetime image (Figure 9). This image does show clearly that there is a diffused signal in the 0% and 60%, but it does not give a clear insight in the signal in the cell with the 30% nanoparticles. The autofluorescence of the cell is quenched in the staining protocol for the other experiments, this is however not done for the WGA-staining and might

be beneficial to apply in further research. Lifetime does however provide some information on the content of the cell and it is clear that the 60% nanoparticles are in the cytosol as expected. The 0% nanoparticle is also taken up by the cell, but mostly in clusters as the signal is not as diffuse as in the 60%. This is similar the results found by N.M. Hamelmann et al. [14].

4.4 Effect of nanoparticles on α-synuclein aggregation

In this research, nanoparticles are added to the cells via cellular uptake and electroporation. In this section, the difference between these two techniques is discussed, as well as the visibility of the nanoparticles and the α-synuclein clusters.

The biggest difference between the uptake and electroporation is the method, but the nanoparticle concentration is also five times higher in the cells that take up the nanoparticles naturally. There are more nanoparticle clusters seen in the uptake, which is very logical as the nanoparticles can cluster by coming into contact with the medium. There are also some clusters in the electroporated cell population, this can be caused by cellular uptake after the electroporation, by already clustered nanoparticles or by clustering in the cytosol. The amount of clusters is however lower than in the cells that only took up nanoparticles naturally. The biggest difference is seen in the 60%, quite some particles were taken up by the cells and thus not washed away with the staining. Due to the high concentration of nanoparticle, it is very probable that nanoparticles clustered as the 60% nanoparticles cluster the most according to the FCS.

Visualisation of the nanoparticles is hard, as some small clusters have a big influence on the normalisation. Due to the clustering, there are a lot of fluorophores at one point, creating a high fluorescent intensity at that point. A logarithmic scale or increasing the intensity during image processing did not work, as this mostly showed autofluorescence and noise. Eliminating signals with a low lifetime might work for further experiments, this is something that can be considered. For the cells with α-synuclein staining, it is vaguely seen that the nanoparticles are in the cell, but it does not show up greatly with the strong red α-synuclein overlay. The uptake of the nanoparticles is however known by the WGA-stain done earlier.

The clusters of α-synuclein are barely seen in the images made in this research, making it questionable if it can be called aggregation. For the cellular uptake, there are small clusters of α-synuclein seen in the cells with the 60% nanoparticles. Next to that, the standard deviation of the average amount of clusters per cell after electroporation is high. Comparing the images in this research with other research on α-synuclein aggregation in cells, shows that the clusters found in this research are very small and hard to notice. Other research is conducted in HEK293 (kidney) and N2a (neuroblastoma) cells, the clusters are significantly bigger, they clearly stand out form the background signal [54, 55]. Some clusters in the cells with the 60% tertiary amine nanoparticle are comparable to the clusters in other research, but these clusters are only visible in a few cells and still relatively small. There are also a lot less clusters than found in other research. The amount of clustering is so unnoticeable that it cannot be stated that the nanoparticles cause aggregation in a reliable way. Next to that, there is barely a difference between the cells with nanoparticles and the control. Only for the 60% it can be said that α-synuclein is possibly somewhat aggregating. Looking at the ThT assay, longer incubation with the nanoparticles might be able to induce visible α-synuclein aggregation. For future research it is also recommended to quantify the size of the α-synuclein aggregates.

4.5 Cell toxicity

The metabolic assay showed that the over-all metabolism decreases for an increasing percentage of tertiary amine. The amount of ROS increases when the amount of tertiary amine in a nanoparticle is higher. In this section, it is discussed how the reliability of these assays can be increased. Secondly, the results are compared to other research and thirdly the the effect of differences in cell number are discussed.

To increase the reliability of the cell toxicity assay, triplicates are better than duplicates. The outer wells have divergent values, it is well known that this can be caused by evaporation (edge effects). This can be prevented by filling the outer wells with for example PBS [56]. It is therefore recommended to do this in future experiments.

N.M. Hamelmann et al. reported a decreasing viability for an increasing percentage of tertiary amine, the concentration used is however much higher and the test in their research took 24 hours. Next to that, they used different cells meaning the expression of α-synuclein is different than in this research [14]. J. Burré et al.

showed a decrease in metabolic activity for cells with mutant α-synuclein compared to only the wild type of α-synuclein. The cells with nanoparticles with a higher amount of tertiary amine show a decreased metabolic activity, this does correlate with the research mentioned. A high amount of tertiary amine is toxic to cells as it can cause membrane permeabilization [57]. There is also barely aggregation seen after 72 hours with nanoparticles in a concentration of 1250 nM, the decrease in metabolic activity and the increase in reactive oxygen species can be caused purely by the toxicity of the nanoparticles and not by the aggregation of α-synuclein. However, the difference in metabolic activity between the cells with different nanoparticles added is bigger than in the research from N.M. Hamelmann et al., meaning that there is probably a combined effect of nanoparticle toxicity and toxicity due to aggregation [14].

Reactive oxygen species are a byproduct of the cell's aerobic activity. They function as signalling molecules, if they are present in a high number oxidative stress arises. ROS are broken down by enzymes, but the absence of ROS homeostasis is linked to Parkinson's disease [58]. Linking the metabolic activity to the amount of cells, is sensitive to big errors [34]. There is of course a correlation, but it can not be ruled out if some cells are just more active than others. In this research, it is assumed the measured metabolic activity (fluorescence intensity) is only dependent on the amount of cells. The amount of ROS is also dependent on the amount of cells and the metabolic activity: if there's less metabolic activity, less ROS should be created [58]. It does however show that nanoparticles with a higher percentage of tertiary amine create more ROS, as it creates more aggregation and thus more oxidative stress [59]. In future research, a life/dead assay might be more beneficial to calculate the amount of cells and correct for this in the metabolic assay and the determination of the amount of ROS.

The relatively low fluorescence intensity as a measure for metabolic activity and the relatively high amount of ROS in the control wells is something to take into account, this makes it seem like the metabolic activity of the cells with the nanoparticles (0% and 30% for the normal cell line, 0% for the FLAG cell line) is higher than the cells without nanoparticles. For the FLAG cell line the standard deviation is so high that it can't be concluded if the metabolic activity is higher or lower in the control. For the normal cell line, the metabolic activity is high for the cells nanoparticles are added to. This can be caused by a different amount of cells, possibly less cells are added to the wells or the cells grew slower. It is also a sign of the very moderate toxicity of the 0% and 30% nanoparticles, the metabolic activity is not negatively affected except when there's a high amount of α-synuclein or nanoparticles with a high amount of tertiary amine.

4.6 Further research

It has become clear that nanoparticles can have an influence on the α-synuclein aggregation, especially with a higher percentage of tertiary amine. There are still questions to be answered in the field of PD research in combination with nanomedicine, this section will introduce what can be researched in the future.

Firstly, the critical nanoparticle concentration for inducing α-synuclein aggregation needs to be examined. This can be done by for example a ThT aggregation assay. It is also important to investigate the presence of the nanoparticles in the cytosol by staining the vesicles or lysosomes inside the cell, instead of only the cell membrane. To see the possible effect of nanoparticles on α-synuclein, cells need to be incubated much longer with the nanoparticles. Next to that, differentiation of the SH-SY5Y cells increases the amount of α-synuclein expressed [60]. This can influence the response of the cells on nanoparticles and needs to be researched further. In future research the potential of nanoparticles to induce α-synuclein aggregation needs to be looked at, as it can give information about the possible toxic effect of polymeric nanoparticles used for nanomedicine. In the end, the most important thing is to decrease the amount of PD cases in the world, as it is an increasing problem [1].

5 Conclusion

The goal of this research was to find the effect of charged single chain polymeric nanoparticles on the aggregation of α-synuclein and the viablity of SH-SY5Y cells. It was expected that the nanoparticles would have affinity for α-synuclein and that the nanoparticles would cause aggregation. Next to that, it was expected that more positive nanoparticles would induce more aggregation and are therefore more toxicity to cells.

This hypothesis can be partly accepted. More positive nanoparticles, with a higher percentage of tertiary amine, are more toxic to SH-SY5Y cells. The nanoparticles do also have an affinity for α-synuclein and induce aggregation after 22.6 ± 6.6 (SD) hours for the 60% nanoparticle. The particles with 0% tertiary amine, negatively charged, limit the aggregation of α-synuclein. In the cell, a very low amount of α-synuclein aggregation is visible for the cells with the 60% nanoparticle. For the other nanoparticles, no aggregation is found. The nanoparticles do thus induce aggregation outside of the cell, but not significantly in the cell in 24 and 72 hours.

References

[1] Ou Z, Pan J, Tang S, Duan D, Yu D, Nong H, et al. Global Trends in the Incidence, Prevalence, and Years Lived With Disability of Parkinson's Disease in 204 Countries/Territories From 1990 to 2019. Frontiers in Public Health. 2021;9. doi:10.3389/fpubh.2021.776847.

[2] Dauer W, Przedborski S. Parkinson's Disease: Mechanisms and Models. Neuron. 2003;39(6):889–909. doi:10.1016/S0896-6273(03)00568-3.

[3] Mahmoudi M, Quinlan-Pluck F, Monopoli MP, Sheibani S, Vali H, Dawson KA, et al. Influence of the Physiochemical Properties of Superparamagnetic Iron Oxide Nanoparticles on Amyloid β Protein Fibrillation in Solution. ACS Chemical Neuroscience. 2013 Jan;4(3):475–485. doi:10.1021/cn300196n.

[4] Alabrahim OAA, Azzazy HMES. Polymeric nanoparticles for dopamine and levodopa replacement in Parkinson's disease. Nanoscale Advances. 2022;4(24):5233–5244. doi:10.1039/d2na00524g.

[5] Bendor JT, Logan TP, Edwards RH. The Function of α-Synuclein. Neuron. 2013 Sep;79(6):1044–1066. doi:10.1016/j.neuron.2013.09.004.

[6] Kim DH, Lee J, Mok K, Lee J, Han KH. Salient Features of Monomeric Alpha-Synuclein Revealed by NMR Spectroscopy. Biomolecules. 2020 Mar;10(3):428. doi:10.3390/biom10030428.

[7] Park JH, Burgess JD, Faroqi AH, DeMeo NN, Fiesel FC, Springer W, et al. Alpha-synuclein-induced mitochondrial dysfunction is mediated via a sirtuin 3-dependent pathway. Molecular Neurodegeneration. 2020 Jan;15(1). doi:10.1186/s13024-019-0349-x.

[8] Klementieva O. Glycodendrimers as Potential Multitalented Therapeutics in Alzheimer's Disease. In: Neuroprotection - New Approaches and Prospects. IntechOpen; 2020. doi:10.5772/intechopen.88974.

[9] Gillam JE, MacPhee CE. Modelling amyloid fibril formation kinetics: mechanisms of nucleation and growth. Journal of Physics: Condensed Matter. 2013 aug;25(37):373101. doi:10.1088/0953-8984/25/37/373101.

[10] Domert J, Sackmann C, Severinsson E, Agholme L, Bergström J, Ingelsson M, et al. Aggregated Alpha-Synuclein Transfer Efficiently between Cultured Human Neuron-Like Cells and Localize to Lysosomes. PLOS ONE. 2016 12;11(12):1–16. doi:10.1371/journal.pone.0168700.

[11] Hijaz BA, Volpicelli-Daley LA. Initiation and propagation of α-synuclein aggregation in the nervous system. Molecular Neurodegeneration. 2020 Mar;15(1). doi:10.1186/s13024-020-00368-6.

[12] Patra JK, Das G, Fraceto LF, Campos EVR, del Pilar Rodriguez-Torres M, Acosta-Torres LS, et al. Nano based drug delivery systems: recent developments and future prospects. Journal of Nanobiotechnology. 2018 Sep;16(1). doi:10.1186/s12951-018-0392-8.

[13] Mohammadi S, Nikkhah M. TiO2 Nanoparticles as Potential Promoting Agents of Fibrillation of α-Synuclein, a Parkinson's Disease-Related Protein. Iranian Journal of Biotechnology. 2017 Aug;15(2):87–94. doi:10.15171/ijb.1519.

[14] Hamelmann NM, Paats JWD, Paulusse JMJ. Cytosolic Delivery of Single-Chain Polymer Nanoparticles. ACS Macro Letters. 2021 Nov;10(11):1443–1449. doi:10.1021/acsmacrolett.1c00558.

[15] Bai Y, Xing H, Wu P, Feng X, Hwang K, Lee JM, et al. Chemical Control over Cellular Uptake of Organic Nanoparticles by Fine Tuning Surface Functional Groups. ACS Nano. 2015;9(10):10227–10236. doi:10.1021/acsnano.5b03909.

[16] Albert K, Kälvälä S, Hakosalo V, Syvänen V, Krupa P, Niskanen J, et al. Cellular Models of Alpha-Synuclein Aggregation: What Have We Learned and Implications for Future Study. Biomedicines. 2022 Oct;10(10):2649. doi:10.3390/biomedicines10102649.

[17] Xicoy H, Wieringa B, Martens GJM. The SH-SY5Y cell line in Parkinson's disease research: a systematic review. Molecular Neurodegeneration. 2017 Jan;12(1). doi:10.1186/s13024-017-0149-0.

[18] Kovalevich J, Langford D. Considerations for the Use of SH-SY5Y Neuroblastoma Cells in Neurobiology. In: Neuronal Cell Culture. Humana Press; 2013. p. 9–21. doi:10.1007/978-1-62703-640-5_2.

[19] Kröger APP, Paats JWD, Boonen RJEA, Hamelmann NM, Paulusse JMJ. Pentafluorophenyl-based single-chain polymer nanoparticles as a versatile platform towards protein mimicry. Polymer Chemistry. 2020;11(37):6056–6065. doi:10.1039/d0py00922a.

[20] Yu L, Lei Y, Ma Y, Liu M, Zheng J, Dan D, et al. A Comprehensive Review of Fluorescence Correlation Spectroscopy. Frontiers in Physics. 2021 Apr;9. doi:10.3389/fphy.2021.644450.

[21] Shao W, Sharma R, Clausen MH, Scheller HV. Microscale thermophoresis as a powerful tool for screening glycosyltransferases involved in cell wall biosynthesis. Plant Methods. 2020 Jul;16(1). doi:10.1186/s13007-020-00641-1.

[22] Jerabek-Willemsen M, André T, Wanner R, Roth HM, Duhr S, Baaske P, et al. MicroScale Thermophoresis: Interaction analysis and beyond. Journal of Molecular Structure. 2014 Dec;1077:101–113. doi:10.1016/j.molstruc.2014.03.009.

[23] Semerdzhiev SA, Dekker DR, Subramaniam V, Claessens MMAE. Self-Assembly of Protein Fibrils into Suprafibrillar Aggregates: Bridging the Nano- and Mesoscale. ACS Nano. 2014;8(6):5543–5551. doi:10.1021/nn406309c.

[24] Xue C, Lin TY, Chang D, Guo Z. Thioflavin T as an amyloid dye: fibril quantification, optimal concentration and effect on aggregation. Royal Society Open Science. 2017 Jan;4(1):160696. doi:10.1098/rsos.160696.

[25] Wördehoff M, Hoyer W. α-Synuclein Aggregation Monitored by Thioflavin T Fluorescence Assay. BIO-PROTOCOL. 2018;8(14). doi:10.21769/bioprotoc.2941.

[26] Emde B, Heinen A, Gödecke A, Bottermann K. Wheat germ agglutinin staining as a suitable method for detection and quantification of fibrosis in cardiac tissue after myocardial infarction. European Journal of Histochemistry. 2014 Dec. doi:10.4081/ejh.2014.2448.

[27] el Biari K, Ángel Gaudioso, Fernández-Alonso MC, Jiménez-Barbero J, Cañada FJ. Peptidoglycan Recognition by Wheat Germ Agglutinin. A View by NMR. Natural Product Communications. 2019;14(5):1934578X19849240. doi:10.1177/1934578X19849240.

[28] Kanazawa T, Takematsu H, Yamamoto A, Yamamoto H, Kozutsumi Y. Wheat germ agglutinin stains dispersed post-golgi vesicles after treatment with the cytokinesis inhibitor psychosine. Journal of Cellular Physiology. 2008;215(2):517–525. doi:10.1002/jcp.21328.

[29] Ramoino P, Fronte P, Fato M, Beltrame F, Robello M, Diaspro A. Fluid phase and receptor-mediated endocytosis in Paramecium primaurelia by fluorescence confocal laser scanning microscopy. European Biophysics Journal. 2001 Sep;30(5):305–312. doi:10.1007/s002490100166.

[30] Sacui I, Szmacinski H, Blair DL, Urbach JS, Zammarano M, Gilman JW. Imaging Cellulose Nanocrystals. Microscopy and Microanalysis. 2013 Aug;19(S2):1870–1871. doi:10.1017/s1431927613011343.

[31] Chacko JV, Eliceiri KW. Autofluorescence lifetime imaging of cellular metabolism: Sensitivity toward cell density, pH, intracellular, and intercellular heterogeneity. Cytometry Part A. 2018 Oct;95(1):56–69. doi:10.1002/cyto.a.23603.

[32] van Uitert I. Investigating cellular electroporation using planar membrane models and miniaturized devices [PhD thesis]. University of Twente. Netherlands; 2010. doi:10.3990/1.9789036530934.

[33] Lonza Knowledge Center. SH-SY5Y; 2016. Accessed 5-6-2023. Available from: https://knowledge.lonza.com/cell?id=132&search=shsy5y.

[34] Braissant O, Astasov-Frauenhoffer M, Waltimo T, Bonkat G. A Review of Methods to Determine Viability, Vitality, and Metabolic Rates in Microbiology. Frontiers in Microbiology. 2020 Nov;11. doi:10.3389/fmicb.2020.547458.

[35] Csepregi R, Lemli B, Kunsági-Máté S, Szente L, Köszegi T, Németi B, et al. Complex Formation of Resorufin and Resazurin with β-Cyclodextrins: Can Cyclodextrins Interfere with a Resazurin Cell Viability Assay? Molecules. 2018 Feb;23(2):382. doi:10.3390/molecules23020382.

[36] del Río LA, Sandalio LM, Corpas FJ, Palma JM, Barroso JB. Reactive Oxygen Species and Reactive Nitrogen Species in Peroxisomes. Production, Scavenging, and Role in Cell Signaling. Plant Physiology. 2006 Jun;141(2):330–335. doi:10.1104/pp.106.078204.

[37] Cominacini L, Pasini AF, Garbin U, Davoli A, Tosetti ML, Campagnola M, et al. Oxidized Low Density Lipoprotein (ox-LDL) Binding to ox-LDL Receptor-1 in Endothelial Cells Induces the Activation of NF-κB through an Increased Production of Intracellular Reactive Oxygen Species. Journal of Biological Chemistry. 2000 Apr;275(17):12633–12638. doi:10.1074/jbc.275.17.12633.

[38] Miller FJ, Griendling KK. [20] - Functional Evaluation of Nonphagocytic NAD(P)H Oxidases. In: Sen CK, Packer L, editors. Redox Cell Biology and Genetics Part B. vol. 353 of Methods in Enzymology. Academic Press; 2002. p. 220–233.

[39] Berezin MY, Achilefu S. Fluorescence Lifetime Measurements and Biological Imaging. Chemical Reviews. 2010;110(5):2641–2684. doi:10.1021/cr900343z.

[40] In: Lakowicz JR, editor. Quenching of Fluorescence. Boston, MA: Springer US; 2006. p. 277–330. doi:10.1007/978-0-387-46312-4_8.

[41] Bae W, Yoon TY, Jeong C. Direct evaluation of self-quenching behavior of fluorophores at high concentrations using an evanescent field. PLOS ONE. 2021 Feb;16(2):e0247326. doi:10.1371/journal.pone.0247326.

[42] Byrdin M, Duan C, Bourgeois D, Brettel K. A Long-Lived Triplet State Is the Entrance Gateway to Oxidative Photochemistry in Green Fluorescent Proteins. Journal of the American Chemical Society. 2018 Feb;140(8):2897–2905. doi:10.1021/jacs.7b12755.

[43] Moore TL, Rodriguez-Lorenzo L, Hirsch V, Balog S, Urban D, Jud C, et al. Nanoparticle colloidal stability in cell culture media and impact on cellular interactions. Chemical Society Reviews. 2015;44(17):6287–6305. doi:10.1039/c4cs00487f.

[44] Rausch K, Reuter A, Fischer K, Schmidt M. Evaluation of Nanoparticle Aggregation in Human Blood Serum. Biomacromolecules. 2010 Oct;11(11):2836–2839. doi:10.1021/bm100971q.

[45] Foroozandeh P, Aziz AA. Insight into Cellular Uptake and Intracellular Trafficking of Nanoparticles. Nanoscale Research Letters. 2018 Oct;13(1). doi:10.1186/s11671-018-2728-6.

[46] Kettler K, Veltman K, van de Meent D, van Wezel A, Hendriks AJ. Cellular uptake of nanoparticles as determined by particle properties, experimental conditions, and cell type. Environmental Toxicology and Chemistry. 2014 Jan;33(3):481–492. doi:10.1002/etc.2470.

[47] Kastritis PL, Moal IH, Hwang H, Weng Z, Bates PA, Bonvin AMJJ, et al. A structure-based benchmark for protein-protein binding affinity. Protein Science. 2011 Feb;20(3):482–491. doi:10.1002/pro.580.

[48] Álvarez YD, Fauerbach JA, Pellegrotti JV, Jovin TM, Jares-Erijman EA, Stefani FD. Influence of Gold Nanoparticles on the Kinetics of α-Synuclein Aggregation. Nano Letters. 2013 Nov;13(12):6156–6163. doi:10.1021/nl403490e.

[49] Tran CH, Saha R, Blanco C, Bagchi D, Chen IA. Modulation of α-Synuclein Aggregation In Vitro by a DNA Aptamer. Biochemistry. 2022 Aug;61(17):1757–1765. doi:10.1021/acs.biochem.2c00207.

[50] Ohgita T, Namba N, Kono H, Shimanouchi T, Saito H. Mechanisms of enhanced aggregation and fibril formation of Parkinson's disease-related variants of α-synuclein. Scientific Reports. 2022 Apr;12(1). doi:10.1038/s41598-022-10789-6.

[51] Dada ST, Hardenberg MC, Toprakcioglu Z, Mrugalla LK, Cali MP, McKeon MO, et al. Spontaneous nucleation and fast aggregate-dependent proliferation of α-synuclein aggregates within liquid condensates at neutral pH. Proceedings of the National Academy of Sciences. 2023 Feb;120(9). doi:10.1073/pnas.2208792120.

[52] Allen RD, Schroeder CC, Fok AK. Intracellular binding of wheat germ agglutinin by Golgi complexes, phagosomes, and lysosomes of Paramecium multimicronucleatum. Journal of Histochemistry & Cytochemistry. 1989 Feb;37(2):195–202. doi:10.1177/37.2.2911005.

[53] Yang L, Zhou Y, Zhu S, Huang T, Wu L, Yan X. Detection and Quantification of Bacterial Autofluorescence at the Single-Cell Level by a Laboratory-Built High-Sensitivity Flow Cytometer. Analytical Chemistry. 2012 Jan;84(3):1526–1532. doi:10.1021/ac2031332.

[54] Paxinou E, Chen Q, Weisse M, Giasson BI, Norris EH, Rueter SM, et al. Induction of α-Synuclein Aggregation by Intracellular Nitrative Insult. The Journal of Neuroscience. 2001 Oct;21(20):8053–8061. doi:10.1523/jneurosci.21-20-08053.2001.

[55] Burré J, Sharma M, Südhof TC. Definition of a Molecular Pathway Mediating α-Synuclein Neurotoxicity. The Journal of Neuroscience. 2015 Apr;35(13):5221–5232. doi:10.1523/jneurosci.4650-14.2015.

[56] Auld DS, Coassin PA, Coussens NP, Hensley P, Klumpp-Thomas C, Michael S, et al. In: Grossman A, Brimacombe K, editors. Microplate Selection and Recommended Practices in High-throughput Screening and Quantitative Biology. Bethesda (MD): Eli Lilly & Company and the National Center for Advancing Translational Sciences; 2020. p. 2004–. Available from: `https://www.ncbi.nlm.nih.gov/books/NBK558077/`.

[57] Sprouse D, Reineke TM. Investigating the Effects of Block versus Statistical Glycopolycations Containing Primary and Tertiary Amines for Plasmid DNA Delivery. Biomacromolecules. 2014 Jun;15(7):2616–2628. doi:10.1021/bm5004527.

[58] Sies H, Jones DP. Reactive oxygen species (ROS) as pleiotropic physiological signalling agents. Nature Reviews Molecular Cell Biology. 2020 Mar;21(7):363–383. doi:10.1038/s41580-020-0230-3.

[59] Puspita L, Chung SY, won Shim J. Oxidative stress and cellular pathologies in Parkinson's disease. Molecular Brain. 2017 Nov;10(1). doi:10.1186/s13041-017-0340-9.

[60] Hasegawa T, Matsuzaki M, Takeda A, Kikuchi A, Akita H, Perry G, et al. Accelerated α-synuclein aggregation after differentiation of SH-SY5Y neuroblastoma cells. Brain Research. 2004 Jul;1013(1):51–59. doi:10.1016/j.brainres.2004.04.018.